HHS Public Access

Author manuscript

Nature. Author manuscript; available in PMC 2016 August 18.

Published in final edited form as:

Nature. 2016 February 18; 530(7590): 336–339. doi:10.1038/nature16938.

Polygenic evolution of a sugar specialization tradeoff in yeast

Jeremy I. Roop[1], **Kyu Chul Chang**[2,3], and **Rachel B. Brem**[1,3]

[1]Department of Plant and Microbial Biology, University of California, Berkeley, Berkeley, California 94720

[2]Department of Molecular and Cell Biology, University of California, Berkeley, Berkeley, California 94720

[3]Buck Institute for Research on Aging, Novato, California, 94945

Abstract

The evolution of novel traits can involve many mutations scattered throughout the genome[1,2]. Detecting and validating such a suite of alleles, particularly if they arose long ago, remains a key challenge in evolutionary genetics[1-3]. Here we dissect an evolutionary tradeoff of unprecedented genetic complexity between long-diverged species. When cultured in 1% glucose medium supplemented with galactose, *Saccharomyces cerevisiae*, but not *S. bayanus* or other *Saccharomyces* species, delayed commitment to galactose metabolism until glucose was exhausted. Promoters of seven galactose (*GAL*) metabolic genes from *S. cerevisiae*, when introduced together into *S. bayanus*, largely recapitulated the delay phenotype in 1% glucose-galactose medium, and most had partial effects when tested in isolation. Variation in *GAL* coding regions also contributed to the delay when tested individually in 1% glucose-galactose medium. When combined, *S. cerevisiae GAL* coding regions gave rise to profound growth defects in the *S. bayanus* background. In medium containing 2.5% glucose supplemented with galactose, wild-type *S. cerevisiae* repressed *GAL* gene expression and had a robust growth advantage relative to *S. bayanus*; transgenesis of *S. cerevisiae GAL* promoter alleles or *GAL* coding regions was sufficient for partial reconstruction of these phenotypes. *S. cerevisiae GAL* genes thus encode a regulatory program of slow induction and avid repression, and a fitness detriment during the glucose-galactose transition but a benefit when glucose is in excess. Together, these results make clear that genetic mapping of complex phenotypes is within reach, even in deeply diverged species.

A central goal of evolutionary genetics is to understand how organisms acquire phenotypic novelties. Such traits, if they have evolved over long timescales, can have a genetic basis quite distinct from those arisen more recently[4]. In landmark cases, single genes underlying species differences have been pinpointed and validated[5], but the polygenic architecture of ancient traits has remained a mystery.

Author Contributions

J.I.R. and R.B.B designed experiments, J.I.R and K.C.C. conducted experiments, J.I.R analyzed data, and J.I.R. and R.B.B wrote the paper.

The authors declare no competing financial interests.

In hybrids formed by mating *Saccharomyces cerevisiae* with other *Saccharomyces* species[6], we noted a pattern of coherent, *cis*-regulatory variation in the seven genes of the galactose metabolic pathway. During growth in medium with glucose as the sole carbon source, the *S. cerevisiae* allele at each *GAL* gene conferred low expression relative to other *Saccharomyces*, except for the repressor *GAL80*, at which the *S. cerevisiae* allele drove expression up (Figure 1b). Likewise, purebred *S. cerevisiae* expressed *GAL* effectors at low levels in glucose, and *GAL80* at high levels, relative to other species (Figure 1b and ref. 7). *S. paradoxus*, the sister species to *S. cerevisiae*, had an intermediate expression phenotype (Figure 1b). Thus, the *S. cerevisiae GAL* program is one of heightened glucose repression relative to other species, as a product of *cis*-regulatory changes at the five loci that encode the seven *GAL* genes. Because such a pattern is unlikely under neutrality[8], these data raised the possibility that selective pressure on the *GAL* pathway had changed along the *S. cerevisiae* lineage.

In *S. cerevisiae*, pre-expression of metabolic genes in glucose medium can boost fitness upon a switch to other carbon sources[9-11]. We therefore expected that *GAL* expression divergence in glucose could have phenotypic correlates in other conditions. Culturing cells in 1% glucose medium supplemented with galactose, we observed a qualitative distinction between species (Figure 2a). In *S. cerevisiae*, growth was retarded by a diauxic lag midway through the timecourse, reflecting the expected delay in assembling galactose metabolic machinery once glucose is exhausted[9,10,12]. In more distantly related yeasts, we observed no lag in 1% glucose-galactose medium supplemented with galactose (Figure 2a-b), although *S. paradoxus* had a modest lag (Figure 2a-b) that echoed its intermediate regulatory phenotype (Figure 1b). Glucose mixtures with maltose and raffinose engendered a lag in all members of the clade (Extended Data Figure 1). *S. cerevisiae* strains from distinct populations all exhibited a lag in glucosegalactose cultures (Figure 2c). These data highlight *S. cerevisiae* as an extreme among *Saccharomyces* with respect to two attributes of galactose metabolism: reduced *GAL* gene expression during growth in pure glucose, and diauxic lag in 1% glucose-galactose medium supplemented with galactose.

To dissect further the divergence in galactose metabolic behaviors, we focused on a comparison of *S. cerevisiae* with its distant relative *S. bayanus* var. *uvarum (S. bayanus)*. In 1% glucose-galactose medium, both species initially metabolized glucose with similar rates, indicating that neither used the sugars simultaneously (Figure 2d). In *S. bayanus* cultures, galactose consumption began at a point just before the complete exhaustion of glucose. For *S. cerevisiae*, glucose exhaustion triggered the diauxic lag, during which galactose levels in its culture medium were largely unchanged. After the lag, with the eventual resumption of log-phase growth by *S. cerevisiae*, galactose levels finally dropped (Figure 2d). These results implicate the transition between glucose and galactose metabolism as a nexus of phenotypic differences between the species.

For direct tests of the phenotypic impact of divergence at the *GAL* genes, we replaced *GAL* gene sequences in one species by those of the other at the endogenous loci (Figure 3a). In a first investigation of *GAL* promoters, *S. cerevisiae* alleles of the regions upstream of *GAL1*, *GAL3*, *GAL4*, and *GAL10* were each sufficient for a partial gain in diauxic lag in *S. bayanus*, in 1% glucose-galactose medium (Figure 3b-c). Control experiments established the inverse

effect of *S. bayanus GAL* promoter alleles, reducing lag in the *S. cerevisiae* background (Extended Data Figure 2).

We next aimed at a more complete reconstruction of *S. cerevisiae*-like galactose metabolic behaviors, which we inferred to be derived, in *S. bayanus* as a representative of the likely ancestral state. An *S. bayanus* strain harboring all seven *GAL* promoters from *S. cerevisiae* recapitulated 69% of the lag phenotype of the *S. cerevisiae* parent (Figure 3b-c), with *GAL* gene expression peaking at the same timepoint as that of wild-type *S. cerevisiae* and at similar amplitude (Figure 3d). Comparison to the sum of lag effects from individual promoter swaps revealed negative epistasis in the seven-promoter replacement strain (Figure 3c), and in strains harboring intermediate *S. cerevisiae* promoter combinations (Extended Data Figure 3).

Transgenesis of individual *S. cerevisiae GAL* coding regions was also sufficient for a partial lag in *S. bayanus*, in the case of *GAL1*, *GAL3*, and *GAL4* (Figure 3b-c). Swaps of *GAL* promoter-coding fusions revealed negative epistasis at *GAL1* and *GAL3*: for these genes, the sum of phenotypes from the respective promoter- and coding transgenics was far more dramatic than the effect of the promoter-coding fusion (Figure 3c). Combining all seven *S. cerevisiae GAL* coding or promoter-coding regions in *S. bayanus*, we observed an exaggerated, long-term growth delay in 1% glucose-galactose medium, distinct from the temporary lag of wild-type strains and promoter transgenics (Figure 3b). This defect reflected dysfunction of multiple modules of the *S. cerevisiae GAL* pathway in *S. bayanus*, as it could be elicited by just the two regulators Gal3 and Gal4 swapped from *S. cerevisiae*, or just *S. cerevisiae* alleles of the enzymes Gal1, Gal7, and Gal10 (Extended Data Figure 3). Coding and promoter-coding swap strains did ultimately resume active growth (Figure 3b) and metabolize galactose from mixed-sugar medium (Extended Data Figure 4), and their *GAL* expression induction was markedly delayed (Figure 3d). These strains also grew poorly in pure galactose medium (Extended Data Figure 5). Together, our data make clear that diauxic lag in 1% glucosegalactose medium can be largely recapitulated by divergent *GAL* gene promoters; *GAL* protein alleles from *S. cerevisiae* make a partial contribution to lag when tested in isolation and, when combined in *S. bayanus*, confer growth defects far exceeding those of either wild-type.

In light of the conservation of diauxic lag across *S. cerevisiae* (Figure 2c), we hypothesized that this species had maintained its divergent galactose metabolic behavior on the basis of a fitness benefit. Among the potential mechanisms for such an advantage, we focused on the possibility that as *S. cerevisiae* represses *GAL* genes in glucose-replete conditions (Figure 1), it avoids the liability of expressing unused proteins and enables rapid growth[10,13]. When cultured in 2.5% glucose medium also containing galactose, wild-type *S. cerevisiae* exhibited a 10% faster growth rate (Figure 4a-b), and 4-9 fold lower expression of *GAL* enzymes (Figure 4c), than *S. bayanus*. Both species metabolized glucose almost exclusively across the timecourse (Figure 4d-e). Replacement of all seven *S. bayanus GAL* promoters with *S. cerevisiae* alleles recapitulated the program of low *GAL* gene expression (Figure 4c), and conferred a growth rate halfway between those of the wild-type species (Figure 4a-b), in 2.5% glucose medium supplemented with galactose. The *S. bayanus* strain harboring all seven *S. cerevisiae GAL* coding regions also expressed *GAL* genes at low levels (Figure 4c),

which mirrored this strain's exaggerated delay in *GAL* gene induction (Figure 3b-d), and was associated with a partial growth benefit (Figure 4a-b). Promoter-coding replacement conferred no additional phenotype over and above the effects of transgenesis of either region type alone (Figure 4a-c). We conclude that *S. cerevisiae GAL* promoters, by shutting down expression of the galactose metabolic pathway, are adaptive in conditions of abundant glucose, and this program can be phenocopied by *S. cerevisiae GAL* protein alleles in *S. bayanus*. Sequence analyses revealed a high ratio of inter-specific divergence to intra-species polymorphism in *GAL* gene promoters, though not in *GAL* coding regions (Extended Data Tables 1-3), suggestive of a history of directional evolution at these loci.

In this work, we have dissected glucose-specialist phenotypes that distinguish *S. cerevisiae* from other members of the *Saccharomyces* clade. *S. cerevisiae* is reluctant to transition from glucose to galactose metabolism, and has a growth advantage in a high-glucose environment. Additionally, the *S. cerevisiae* program confers an increase in biomass accumulation during growth in pure galactose (Extended Data Figure 5c) and could also be beneficial when glucose availability fluctuates rapidly[11]. As *S. cerevisiae* alleles of *GAL* gene promoters are largely sufficient for this family of traits, they may have served as an easily evolvable, and likely adaptive, origin of these characters. By contrast, the *S. cerevisiae GAL* proteome, which confers synthetic growth defects in modern-day *S. bayanus*, may have evolved slowly over a rugged fitness landscape, under distinct forces or at a different period. Such a model would dovetail with the *cis*-regulatory basis of a related, but genetically simple, galactose metabolism trait that evolved more recently between yeasts[13]. For any suite of divergent regulatory regions, observing *cis*-acting effects on gene expression can open a first window onto their phenotypic relevance and that of the gene products they control. With this paradigm, evolutionary biologists need not be limited by polygenicity in the mapping of genotype to phenotype, even between long-diverged species.

Materials and methods

Yeast strains

Strains used in this study are listed in Supplementary Table 1. Abbreviations in figures and tables are as follows: S. cer, Saccharomyces cerevisiae; S. par, Saccharomyces paradoxus; S. mik, Saccharomyces mikatae; S. bay, Saccharomyces bayanus; S. cas, Saccharomyces castellii. Allele-swap strains constructed in haploid *S. bayanus* JRY294 or JRY296 (isogenic MATa and MATα derivatives of type strain CBS7001) used the MIRAGE method[14] with several modifications as follows. A 1.7kb region containing the *K. lactis* URA3 coding sequence and regulatory region was amplified from the pCORE-UH plasmid[15] and used for each half of the inverted repeat. The *S. cerevisiae GAL* region to be swapped in was attached to one half of the inverted repeat cassette by overlap extension PCR, after which the two halves of the final cassette were ligated together. Due to the different sizes of the two halves of the inverted repeat cassette, a second restriction digestion step as described in ref. 14 was not necessary to remove non-desired ligation products. Transformation with the cassette, followed by confirmation of positive transformants and plating onto 5-FOA medium, resulted in excision of the inverted repeat from the target genome, leaving behind a marker-less allele swap at the locus. Sanger sequencing was used to verify the correct nucleotide

sequence of each swapped allele. The *S. cerevisae* allele of each promoter and CDS was amplified from genomic DNA of YHL068 (ref. 6). Promoter, coding, and promoter-coding fusion swap strains were engineered by replacing 600bp of intergenic region directly upstream of the CDS, the CDS, or these two regions combined, respectively, in *S. bayanus* with orthologous regions from *S. cerevisiae*. For allele swaps in the *S. cerevisiae* background in Extended Data Figure 2, 720bp of the region between the *GAL1* and *GAL10* open reading frames was amplified from *S. bayanus* strain CBS7001 and used to construct a MIRAGE cassette as above, and transformed into *S. cerevisiae* strain JRY313 (isogenic MATa derivative of BY4743) and selected as above. For each transgenic, two or more independent transformants were used as replicates for growth profiling and sugar concentration measurements. Combining unlinked allele swaps into a single genome was accomplished by single-cell mating of single-locus swaps, followed by sporulation, tetrad dissection, and diagnostic PCR to identify segregant colonies with the allele combinations of interest. *S. cerevisiae* alleles of *GAL1*, *GAL7* and *GAL10* were combined in the *S. bayanus* background by successive allele swap transformations.

Growth curves and quantification

All growth experiments were conducted at 26°C in YP media (2% bacto-peptone, 1% yeast extract) supplemented with various carbon sources as follows. Experiments measuring diauxic lag in 1% glucose medium supplemented with galactose utilized medium containing 1% glucose and 1% galactose. Experiments measuring growth profiles in other non-galactose carbon sources utilized media containing 1% glucose and 1% of the secondary carbon source as indicated. Experiments measuring maximum growth rates in high-glucose media containing galactose utilized medium containing 2.5% glucose and 10% galactose. Experiments measuring growth profiles in pure galactose medium utilized media containing 2% galactose.

Growth timecourses were carried out as follows. Strains were grown in YP containing 2% galactose (Figure 4 and Extended Data Figure 5) or 2% glucose (all other figures) for 24 hours with shaking at 200rpm. Each strain was then back-diluted into the same medium to an OD of 0.1 and grown for an additional 6 hours. These log-phase cultures were then back-diluted to an OD of 0.02 in a 96-well plate containing 150µl of YP with the appropriate amount of a given carbon source. Plates were covered with a gas-permeable membrane, placed in a Tecan F200 plate reader and incubated with orbital shaking for the duration of each experiment. OD_{600} measurements were made every 30 minutes.

Gain in lag was calculated from growth curves as (1 - geometric mean rate) of a given strain. Geometric mean rate (GMR) was calculated as in ref. 11, with the following differences. A window of 0.1 to 0.8 OD units was used for quantification in all figures apart from Figure 2b. In Figure 2b, GMR was calculated within a window bounded by 20% and 80% of the maximum final yield attained during the time course for each species. Maximum growth rate was calculated as in ref. 10 except that a window of 0.01 to 0.3 OD units was used and a geometric mean of growth rates was calculated. Final growth yield was calculated as the difference between initial and final OD_{600} measurements as in ref. 16.

Replication schemes and analysis were as follows. To enable qualitative comparisons among species in Figures 2a, 2b and 2c, on a given 96-well plate, six biological replicate cultures of each strain were assayed. On each growth plate, replicate fitness values greater than two standard deviations from the mean of fitness values for that strain were considered artifacts of technical error and discarded. Displayed data for a given strain are the results of growth measurements from one plate and are representative of at least two plates cultured on different days. Experiments in Figure 2d were as in Figure 2a-2c except that four biological replicate cultures were measured.

To enable highly powered quantitative comparisons among strains of growth in 1% glucose-galactose medium in Figure 3b-c, 12 biological replicate cultures of each transgenic strain were assayed across several plates and days, in each case alongside replicates of wild-type *S. bayanus* and *S. cerevisiae*. The growth rate of a given strain measured on a given plate was normalized to the value for wild-type *S. bayanus* on that plate, and these normalized measurements were then averaged across plates. Because we included wild-type strains on each plate, their growth measurements as displayed in Figure 3b-c are averages over 78 and 54 replicates of *S. bayanus* and *S. cerevisiae*, respectively. Artifact filtering was as above. Differences in growth among strains were assessed for statistical significance by a two-sided Wilcoxon rank-sum test and a Bonferroni correction was applied in instances of multiple tests.

To enable highly powered quantitative comparisons among strains of growth in medium containing 2.5% glucose and 10% galactose in Figure 4a-b, we assayed growth of 250, 170, 204, 136, and 192 biological replicate cultures of wild-type *S. bayanus*, wild-type *S. cerevisiae*, the combinatorial promoter transgenic strains, the combinatorial promoter-coding transgenic strains, and the combinatorial coding transgenic strains, respectively, across several plates and days. As above, growth measurements for each strain in turn assayed on a given plate was normalized to the wild-type *S. bayanus* cultured on that plate, and normalized growth rate measurements were combined across plates. Artifact filtering and statistical testing were as above.

Experiments in Extended Data Figure 1 were as in Figure 2a-2c. Experiments for Extended Data Figure 2 were as in Figure 3 except that 12 replicate cultures were measured for each strain. Experiments for Extended Data Figure 3 were as in Figure 3b-c. Experiments for Extended Data Figure 4 were as in Figure 2a-2c.

Sugar measurements

For growth timecourse experiments in which sugar concentration was measured, an appropriate number of wells (see below) were inoculated into a 96-well plate and cultured in the Tecan F200 plate reader as above, such that media from at least two replicate wells could be harvested at each timepoint of interest and at least four replicate cultures of each strain would remain untouched for growth curve analysis. Samples were taken for sugar measurement by cutting the membrane covering the 96-well plate with a razor and extracting all 150μl of cell culture in a given well. Care was taken to only puncture the membrane above the harvested well such that adjacent wells were not affected. Cells and debris were pelleted from the sampled culture by brief centrifugation and the supernatant

was extracted for quantification of glucose and galactose. Glucose was measured using the GlucCell glucose monitoring system (Chemglass Life Sciences). Galactose was measured with the Amplex Red Galactose Oxidase assay kit (Molecular Probes, Life Technologies). For galactose measurements, a Tecan Safire plate reader (Tecan) was used to quantify fluorescence and the relationship between fluorescence and galactose concentration was determined using a standard curve.

Data in Figure 2d were obtained by sampling two biological replicate cultures at each timepoint. Data in Figure 4d, 4e and Extended Data Figure 4 were obtained by sampling three biological replicate cultures at both the start and endpoints of the growth timecourse. For all experiments, three technical replicates were assayed for each biological replicate culture sampled, and mean values are reported. All data are representative of two identical experiments conducted on different days.

Quantitative PCR

Timepoint samples for qPCR analysis were obtained from cultures analogously to those obtained for sugar consumption quantification detailed above. Between two and fifteen replicate wells were harvested at each timepoint and pooled in order to have sufficient biological material for RNA isolation. RNA was isolated using an RNeasy mini kit (Qiagen) and cDNA was synthesized using SuperScript III (Life Technologies). DyNAmo HS SYBR green (Thermo Scientific) was used for quantitative PCR and all quantification was done on a CFX96 machine (BioRad). Gene expression levels relative to *ACT1* were calculated using the $2^{-\Delta\Delta Ct}$ method[17]. Three technical replicates per biological sample were assayed, and mean values are reported. Primer sequences and cycling times are in Supplementary Table 2.

Sequence analyses

Custom Python scripts were used to extract coding sequences and 600bp promoter regions for type strains of *S. paradoxus*, *S. mikatae*, and *S. bayanus*[18] for each gene that had an ortholog in each of the five *Saccharomyces sensu strico* species as reported in ref. 18. *S. cerevisiae* population sequences were downloaded from the following sources:

YJM978, UWOPS83-787, Y55, UWOPS05-217.3, 273614N, YS9, BC187, YPS128, DBVPG6765, YJM975, L1374, DBVPG1106, K11, SK1, 378604X, YJM981, UWOPS87-2421, DBVPG1373, NCYC3601, YPS606, Y12, UWOPS05-227.2, and YS2 from http://www.yeastrc.org/g2p/home.do; Sigma1278b, ZTW1, T7, and YJM789 from http://www.yeastgenome.org/; and RM11 from http://www.broadinstitute.org/annotation/genome/saccharomyces_cerevisiae. *S .cerevisiae* sequences were aligned to each of the other three species in turn using FSA (ref. 19), using the '--nucprot' option for the coding sequence alignments. For each set of species alignments, nucleotide replacement and polymorphic sites were tabulated using Polymorphorama[20] for coding regions and custom Python scripts for promoter regions.

Sequence analyses of the seven genes of the *GAL* pathway (*GAL1*, *GAL2*, *GAL3*, *GAL4*, *GAL7*, *GAL10*, and *GAL80*) using *S. paradoxus*, *S. mikatae*, or *S. bayanus* as an outgroup were done as follows. For a given species comparison, we first calculated the NI_{TG}

statistic[21] for the promoter regions of the *GAL* genes using synonymous sites in the downstream gene as putative neutral sites, as

$$\frac{\sum D_{si}P_{ri}/(P_{si}+D_{si})}{\sum P_{si}D_{ri}/(P_{si}+D_{si})}$$

where *i* counts genes of the group, D_s and D_r denote the number of divergent synonymous and divergent promoter sites respectively, and P_s and P_r denote the number of polymorphic synonymous and polymorphic promoter sites respectively.

Minor alleles with a frequency of less than 0.15 were ignored[22,23] and all site counts were corrected for multiple hits using a Jukes-Cantor model. In computing NI_{TG} for the seven genes of the *GAL* pathway, we considered that since *GAL1* and *GAL10* are adjacent genes on chromosome II sharing a 662bp promoter region, simply counting sites within 600bp promoter regions for each gene separately would have resulted in double-counting of 532bp. To avoid this, we aligned the 662bp intergenic region of these two genes and considered it one locus in the NI_{TG} calculation. Synonymous sites for this region were taken as the sum of such sites in both the *GAL1* and *GAL10* coding sequences. To evaluate significance, we generated 10,000 randomly chosen groups of six genes each and computed NI_{TG} across the promoters of each such null group as above. The empirical significance of the true NI_{TG} value for *GAL* gene promoters was then taken as the proportion of null groups whose promoters gave an NI_{TG} less than or equal to the true value. We assessed selection acting on non-synonymous sites in *GAL* coding sequences with a pipeline analogous to the above, except that *GAL1* and *GAL10* were considered separate loci, as the coding sequences do not overlap; thus our resampling test used 10,000 random groups of seven coding regions each. Tests for selection using the Neutrality Index statistic[24] [(polymorphic non-synonymous sites/polymorphic synonymous sites) / (divergent non-synonymous / divergent synonymous sites), with a similar formulation for non-synonymous sites] used the same pipeline as above except that we tabulated the average NI across genes of a group, and compared this average quantity for the *GAL* genes against resampled groups of the same size.

D_{XY} (ref. 25), the average number of pairwise differences between outgroup species and *S. cerevisiae* strains, and intrapopulation nucleotide diversity[26] (π), were calculated using custom Python scripts. Nucleotide diversity was ascertained on alignments containing only *S. cerevisiae* strains belonging to the European population, the most deeply sampled in our data set. Empirical significance of these statistics for *GAL* gene promotes and coding sequences was calculated using the resampling pipeline described above.

Code availability

Custom Python scripts used for data analysis are available upon request.

Extended Data

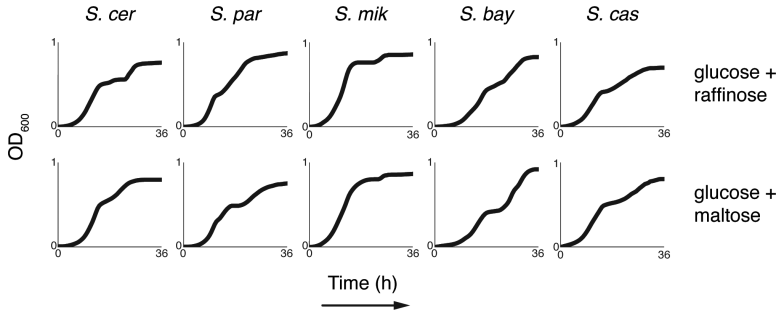

Extended Data Figure 1. Divergence in the *S. cerevisiae* diauxic lag trait is specific to growth in glucose-galactose medium

Each trace reports growth of the indicated yeast inoculated into medium containing 1% glucose and 1% of the indicated secondary carbon source.

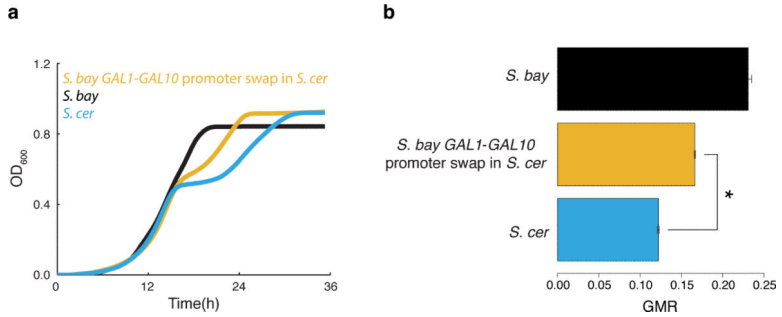

Extended Data Figure 2. The *S. bayanus* allele of the *GAL1* and *GAL10* promoters confers partial rescue of diauxic lag in *S. cerevisiae* in 1% glucose-galactose medium

a) Data are as in Figure 3b of the main text, except that the yellow curve reports growth of an *S. cerevisiae* strain harboring the *GAL1* and *GAL10* promoters from *S. bayanus*. **b)** Each bar reports the geometric mean growth rate (GMR) of the strains shown in **a.** Error bars report standard error of the mean, and the asterisk indicates a significantly different rate ($p < 1 \text{ X } 10^{-15}$, Wilcoxon rank-sum) between the transgenic swap strain and wild-type *S. cerevisiae*.

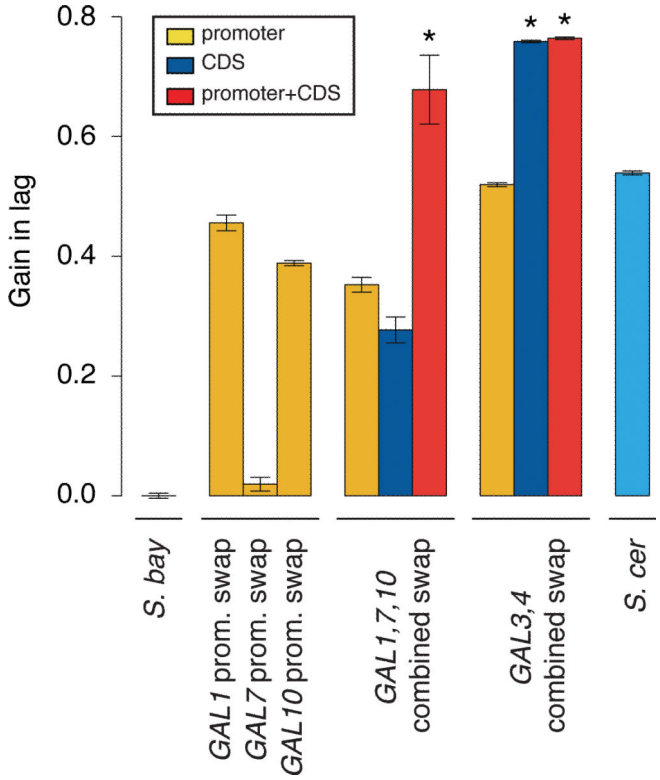

Extended Data Figure 3. Intermediate combinations of *S. cerevisiae GAL* gene alleles confer an exaggerated lag defect on *S. bayanus*, in 1% glucose-galactose medium

Each bar reports the ratio of the GMR to that of wild-type *S. bayanus*, subtracted from 1, from a timecourse of the indicated strain inoculated into medium containing 1% glucose and 1% galactose. The first through fourth bars, and the last bar, are from Figure 3c of the main text; each of the remaining bars reports results from an *S. bayanus* strain harboring *S. cerevisiae* alleles at the indicated combination of *GAL* loci. Symbols and analyses are as in Figure 3c of the main text.

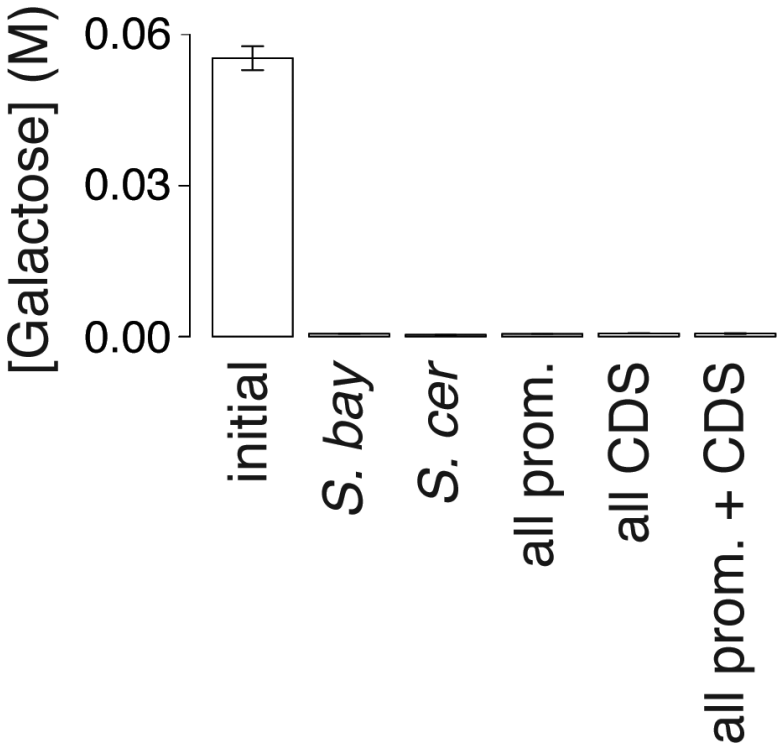

Extended Data Figure 4. *S. bayanus* strains harboring *S. cerevisiae* alleles of all seven *GAL* loci, inoculated into 1% glucose-galactose medium, deplete growth media of galactose

The first bar reports galactose concentration in medium before inoculation, and the remaining bars report concentrations after growth timecourses, in the experiments in Figure 3b of the main text.

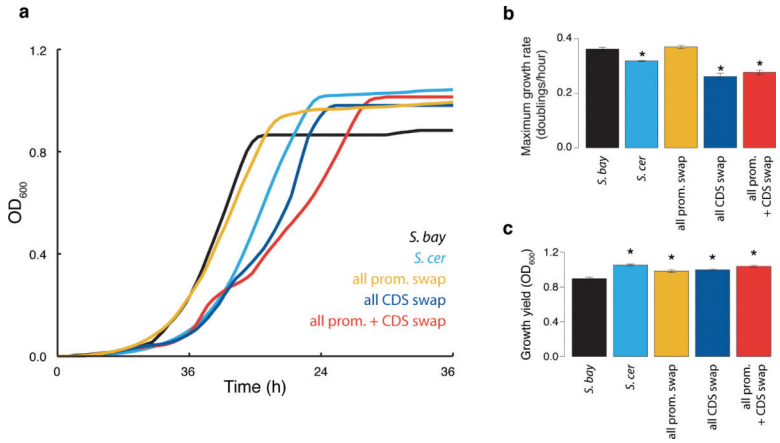

Extended Data Figure 5. In pure galactose medium, *S. cerevisiae* alleles of *GAL* loci are sufficient for increased biomass accumulation and, in the case of protein-coding regions, slow growth

a) Each trace reports growth of an *S. bayanus* strain harboring *S. cerevisiae* alleles of all seven *GAL* genes, or a wild-type control, inoculated into medium containing 2% galactose. **b)** Each bar reports maximum growth rate from the respective timecourse in **a.** Error bars report standard error of the mean, and asterisks indicate values significantly different ($p < 0.05$, Wilcoxon rank-sum) from wild-type *S. bayanus*. **c)** Each bar reports growth yield from

the respective timecourse in **a.** Error bars report standard error of the mean, and asterisks indicate values significantly different ($p < 0.05$, Wilcoxon rank-sum) from wild-type *S. bayanus*.

Extended Data Table 1

Excess of divergence relative to polymorphism in *GAL* promoter regions

Each panel reports analyses of the NI_{TG} measure[21] comparing polymorphism within *S. cerevisiae* to divergence between *S. cerevisiae* and the indicated outgroup species, taken across promoter sites (**a**) or non-synonymous coding sites (**b**), with normalization by the analogous measure from synonymous coding sites. In a given panel, the first row reports NI_{TG} across the seven *GAL* genes, the second row reports the mean NI_{TG} from 10,000 randomly drawn gene groups, and the bottom row reports empirical significance of the distinction between *GAL* genes and the genomic null.

a

	Outgroup		
Statistic	***S. par***	***S. mik***	***S. bay***
NI_{TG} *GAL* promoters	0.32	0.37	0.31
NI_{TG} genome promoters	0.72	0.91	0.73
p-value	0.025	0.013	0.018

b

	Outgroup		
Statistic	***S. par***	***S. mik***	***S. bay***
NI_{TG} *GAL* non-synonymous sites	0.98	0.92	1.03
NI_{TG} genome non-synonymous sites	1.28	1.21	1.27
p-value	0.25	0.19	0.26

Extended Data Table 2

Divergence between species, and polymorphism within *S. cerevisiae*, at *GAL* loci

a) The first line reports mean D_{XY} for *GAL* promoters in comparisons between *S. cerevisiae* and outgroup species. The second line reports the analogous statistics for the mean of 10,000 randomly drawn gene groups, and the third line reports empirical significance of the distinction between *GAL* genes and the genomic null. The fourth, fifth, and sixth lines are analogous to the above except that *GAL* coding regions were analyzed. **b**) The first line reports π for *GAL* promoters or coding regions within *S. cerevisiae*. The second line reports the analogous statistics for the mean of 10,000 randomly drawn gene groups, and the third line reports empirical significance of the distinction between *GAL* genes and the genomic null.

a

	Outgroup		
D_{XY}	***S. par***	***S. mik***	***S. bay***
GAL promoters	0.172	0.276	0.328
genome promoters	0.15	0.241	0.281
p-value	0.147	0.099	0.045
GAL CDS	0.102	0.155	0.188
genome CDS	0.096	0.153	0.190
p-value	0.337	0.429	0.573

b

π	**promoters**	**CDS**
GAL	0.00067	0.00069
genome	0.00194	0.00113
p-value	0.181	0.513

Extended Data Table 3

Evaluation of selection acting on *S. cerevisiae* promoter and coding sequences using the neutrality index statistic

Data are as in Extended Data Table 1 except that the neutrality index[24] was used for each test.

a

	Outgroup		
Statistic	***S. par***	***S. mik***	***S. bay***
GAL promoters	0.32	0.42	0.35
genome promoters	0.94	1.13	0.92
p-value	0.003	0.009	0.014

b

	Outgroup		
Statistic	***S. par***	***S. mik***	***S. bay***
GAL non-synonymous sites	1.43	1.24	1.44
genome non-synonymous sites	2.02	1.88	1.80
p-value	.30	.22	.36

Supplementary Material

Refer to Web version on PubMed Central for supplementary material.

Acknowledgements

This work was supported by NIH GM087432 to R.B.B. and a Hellman Graduate Fellowship from UC Berkeley to J.I.R. The authors thank Adam Arkin for his generosity with advice and resources; Jasper Rine for yeast strains; Ophelia Venturelli for technical expertise; and Avi Flamholz, Josh Schraiber and Patrick Shih for helpful discussions.

References

1. The genetic theory of adaptation: a brief history. 2005; 6:119–127.
2. Rockman MV. THE QTN PROGRAM AND THE ALLELES THAT MATTER FOR EVOLUTION: ALL THAT'S GOLD DOES NOT GLITTER. Evolution. 2012
3. Pritchard JK, Pickrell JK, Coop G. The genetics of human adaptation: hard sweeps, soft sweeps, and polygenic adaptation. Curr. Biol. 2010; 20:R208–15. [PubMed: 20178769]
4. SAVOLAINEN O, Lascoux M, Merilä J. Ecological genomics of local adaptation. Nat. Rev. Genet. 2013; 14:807–820. [PubMed: 24136507]
5. A golden age for evolutionary genetics? Genomic studies of adaptation in natural populations. Trends in Genetics. 2010; 26:484–492. [PubMed: 20851493]
6. Schraiber JG, Mostovoy Y, Hsu TY, Brem RB. Inferring Evolutionary Histories of Pathway Regulation from Transcriptional Profiling Data. PLoS Comput. Biol. 2013; 9:e1003255. [PubMed: 24130471]
7. Caudy AA, et al. A new system for comparative functional genomics of Saccharomyces yeasts. Genetics. 2013; 195:275–287. [PubMed: 23852385]
8. Bullard JH, Mostovoy Y, Dudoit S, Brem RB. Polygenic and directional regulatory evolution across pathways in Saccharomyces. Proc. Natl. Acad. Sci. U.S.A. 2010; 107:5058–5063. [PubMed: 20194736]
9. Venturelli OS, Zuleta I, Murray RM, El-Samad H. Population Diversification in a Yeast Metabolic Program Promotes Anticipation of Environmental Shifts. PLoS Biol. 2015; 13:e1002042. [PubMed: 25626086]
10. Wang J, et al. Natural Variation in Preparation for Nutrient Depletion Reveals a Cost–Benefit Tradeoff. PLoS Biol. 2015; 13:e1002041. [PubMed: 25626068]
11. New AM, et al. Different Levels of Catabolite Repression Optimize Growth in Stable and Variable Environments. PLoS Biol. 2014; 12:e1001764. [PubMed: 24453942]
12. De Deken RH. The Crabtree effect: a regulatory system in yeast. Microbiology (Reading, Engl.). 1966; 44:149–156.
13. Peng W, Liu P, Xue Y, Acar M. Evolution of gene network activity by tuning the strength of negative-feedback regulation. Nat Commun. 2015; 6:1–9.
14. Nair NU, Zhao H. Mutagenic inverted repeat assisted genome engineering (MIRAGE). Nucleic Acids Res. 2009; 37:e9. [PubMed: 19050015]
15. Storici, F.; Resnick, MA. Methods in Enzymology. Vol. 409. Elsevier; 2006. p. 329-345.

16. Warringer J, et al. Trait variation in yeast is defined by population history. PLoS Genetics. 2011; 7:e1002111. [PubMed: 21698134]
17. Livak KJ, Schmittgen TD. Analysis of Relative Gene Expression Data Using Real-Time Quantitative PCR and the 2–ΔΔCT Method. Methods. 2001; 25:402–408. [PubMed: 11846609]
18. Scannell DR, et al. The Awesome Power of Yeast Evolutionary Genetics: New Genome Sequences and Strain Resources for the Saccharomyces sensu stricto Genus. G3 (Bethesda). 2011; 1:11–25. [PubMed: 22384314]
19. Bradley RK, et al. Fast statistical alignment. PLoS Comput. Biol. 2009; 5:e1000392. [PubMed: 19478997]
20. Haddrill PR, Bachtrog D, Andolfatto P. Positive and Negative Selection on Noncoding DNA in Drosophila simulans. Mol Biol Evol. 2008; 25:1825–1834. [PubMed: 18515263]
21. Stoletzki N, Eyre-Walker A. Estimation of the neutrality index. Mol Biol Evol. 2011; 28:63–70. [PubMed: 20837603]
22. Charlesworth J, Eyre-Walker A. The McDonald-Kreitman Test and Slightly Deleterious Mutations. Mol Biol Evol. 2008; 25:1007–1015. [PubMed: 18195052]
23. He BZ, Holloway AK, Maerkl SJ, Kreitman M. Does Positive Selection Drive Transcription Factor Binding Site Turnover? A Test with Drosophila Cis-Regulatory Modules. PLoS Genetics. 2011; 7:e1002053. [PubMed: 21572512]
24. Rand DM, Kann LM. Excess amino acid polymorphism in mitochondrial DNA: contrasts among genes from Drosophila, mice, and humans. Mol Biol Evol. 1996; 13:735–748. [PubMed: 8754210]
25. Nei, M. Molecular Evolutionary Genetics. Columbia University Press; New York: 1987.
26. Nei M, Li WH. Mathematical model for studying genetic variation in terms of restriction endonucleases. Proc. Natl. Acad. Sci. U.S.A. 1979; 76:5269–5273. [PubMed: 291943]

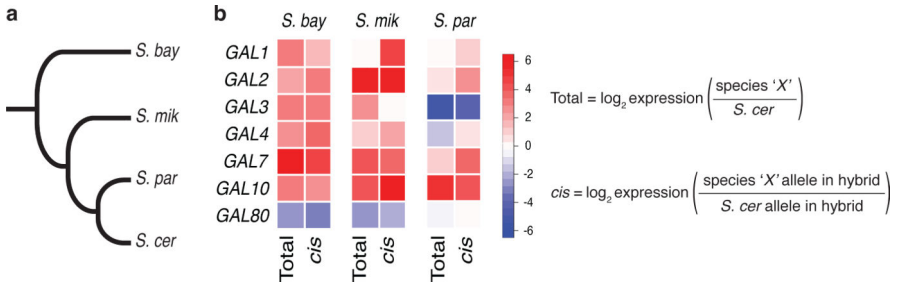

Figure 1. Polygenic *cis*-regulatory evolution among yeast species in galactose metabolic genes

a) Tree of *Saccharomyces* species studied here[18]. **b)** Ratios of expression between the indicated species and *S. cerevisiae*, of the indicated galactose metabolism gene during culture in glucose medium[6]. Total, expression measured in purebred species; *cis*, expression from the indicated species' allele in a diploid hybrid between this species and *S. cerevisiae*, reflecting effects of *cis*-regulatory divergence.

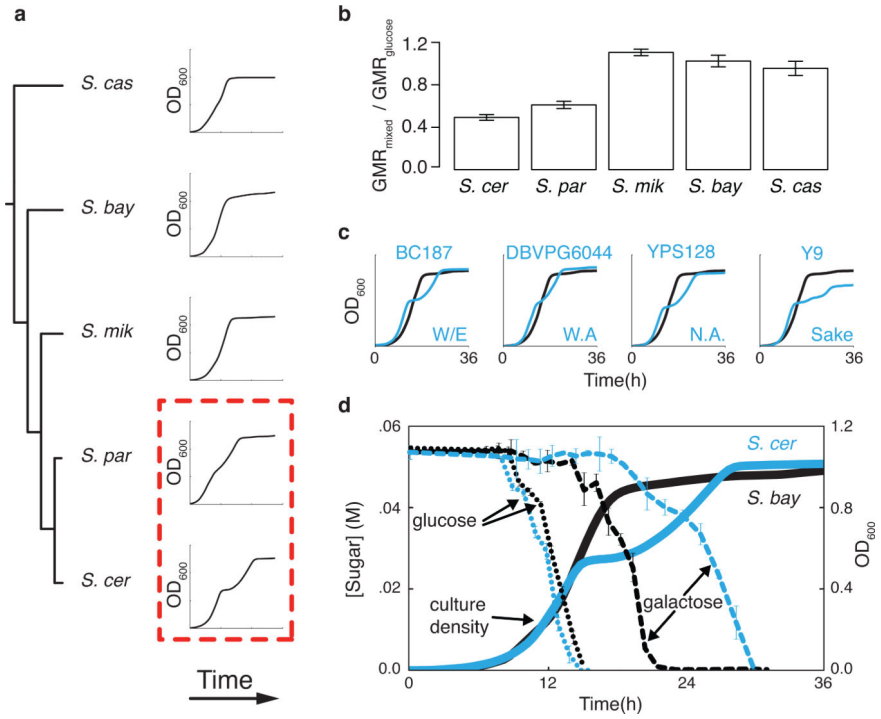

Figure 2. Diauxic lag, in 1% glucose-galactose medium, is conserved within *S. cerevisiae* and divergent among species

a) Growth of *Saccharomyces* type strains inoculated into medium containing 1% glucose and 1% galactose. **b)** Geometric means of the growth rates (GMR) from **a**, normalized to the analogous quantity in glucose medium. **c)** Growth of *S. cerevisiae* isolates (blue) from the indicated populations (W/E, Wine/European; W.A., West African; N.A., North American) and the *S. bayanus* type strain (black), inoculated into medium containing 1% glucose and 1% galactose. **d)** Growth (solid lines) of *S. cerevisiae* and *S. bayanus* inoculated into medium containing 1% glucose and 1% galactose, and medium concentrations of glucose and galactose (dotted and broken lines, respectively). Error bars report standard error of the mean.

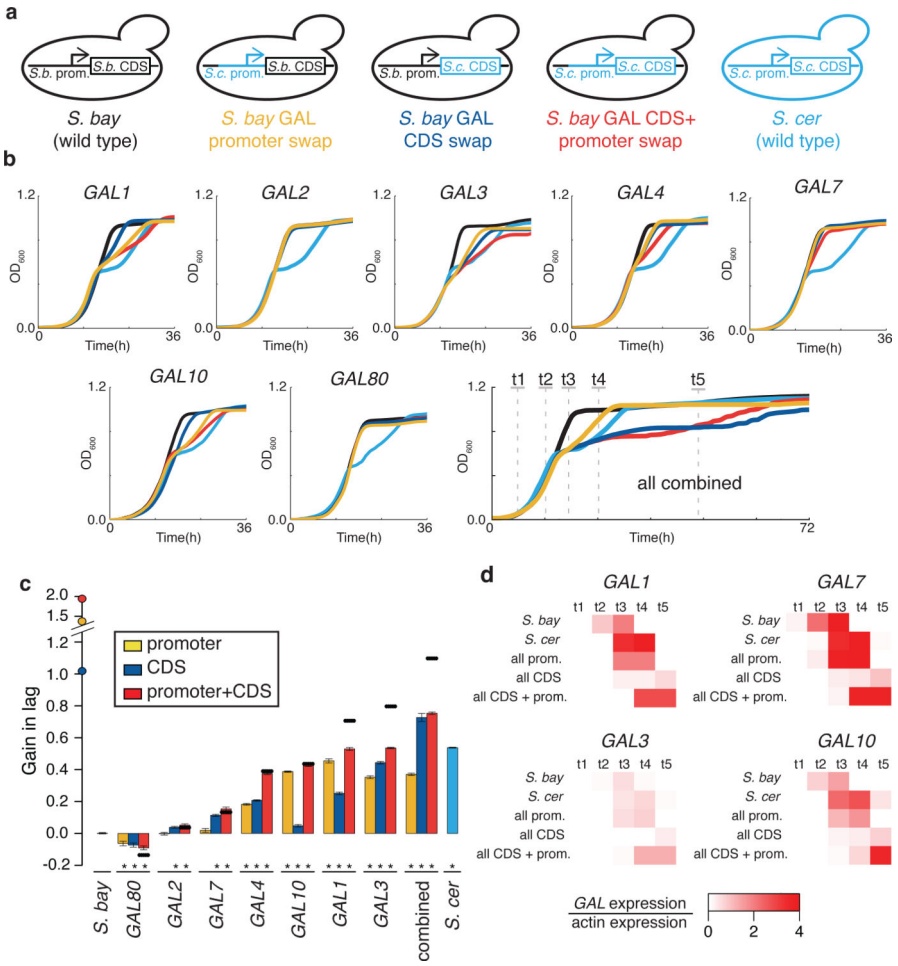

Figure 3. *S. cerevisiae* alleles of *GAL* genes confer diauxic lag in 1% glucose-galactose medium

a) Replacement of *S. cerevisiae GAL* sequences into *S. bayanus* at the endogenous loci. **b)** Growth of *S. bayanus* harboring *S. cerevisiae* alleles of a single *GAL* gene, or of all seven genes, inoculated into medium containing 1% glucose and 1% galactose. **c)** Each bar reports the ratio of the GMR from **b** to that of wild-type *S. bayanus*, subtracted from 1; negative values are GMRs faster than wild-type. Error bars report standard error of the mean. Asterisks, significant differences ($p < 0.001$, Wilcoxon rank-sum) from wild-type *S. bayanus.* Also shown are expected phenotypes of promoter-CDS transgenics for a single gene (horizontal lines) or seven-locus transgenics (circles on *y*-axis), under an additive model of contributions from the regions combined in the respective strains. **d)** *GAL* gene expression at timepoints indicated in the final panel of **b.**

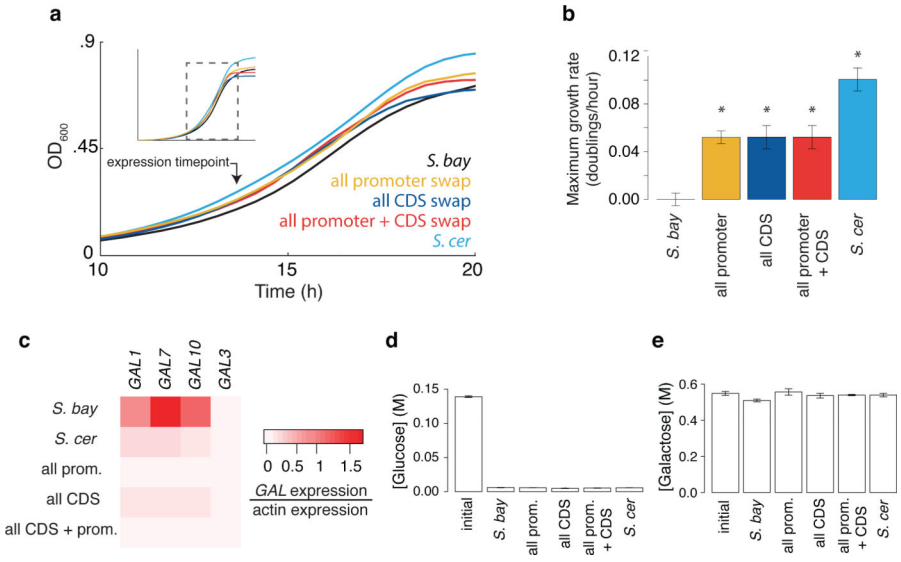

Figure 4. *S. cerevisiae GAL* alleles confer a fitness advantage in 2.5% glucose medium supplemented with galactose

a) Growth of *S. bayanus* strains harboring *S. cerevisiae* alleles of all seven *GAL* genes, and the wild-type species, inoculated into medium containing 2.5% glucose and 10% galactose. **b)** Each bar reports the difference in maximum growth rate between the indicated species and wild-type *S. bayanus* from **a**. Error bars report standard error of the mean, and asterisks indicate rates significantly different ($p < 1 \text{ X } 10^{-8}$, Wilcoxon rank-sum) from wild-type *S. bayanus*. **c)** *GAL* gene expression at the timepoint indicated by the arrow in **a**. **d-e)** In each panel, the first bar reports sugar concentration in medium before inoculation; the remaining bars report sugar concentrations in medium after growth timecourses in **a.**